**Proceedings of the 7th GACM Colloquium on Computational Mechanics**
**for Young Scientists from Academia and Industry**
**October 11-13, 2017 in Stuttgart, Germany**

# Numerical Analysis of Virtualized Heart Models

Barış Cansız[1], Michael Kaliske[1]*, Krunoslav Sveric[2], Karim Ibrahim[2], Ruth Strasser[2]

**Micro Abstract**
Our novel numerical tools simulating cardiac electromechanics will be introduced. The performance and applicability of the framework will be demonstrated through finite element simulations based on real heart geometries. We will compute left ventricular volume-time curves, pressure-volume curves and electrocardiograms. The results will be compared to real clinical data by means of LV motion. The importance of boundary conditions on LV motion will be discussed.

[1]Institute for Structural Analysis, Technische Universität Dresden, Dresden, Germany
[2]Department of Internal Medicine and Cardiology, Heartcenter, Technische Universität Dresden, Dresden, Germany
*__Corresponding author__: michael.kaliske@tu-dresden.de

## Introduction

The human heart is evolved to maintain continuous blood flow through the body thereby supplying essential substrates to every single cell and keeping the whole system functioning. Understanding how a healthy heart functions and how disease develops is one of the most pursued goal by both clinicians and engineers with an aim to achieve robust diagnostic tools and precise patient-specific treatment strategies. However, the challenges in vivo experiments, unique properties and conditions of each patient's make demanding to establish general consensus on diagnosis and treatment methods. In this contribution, we present our recently developed numerical framework towards patient-specific computer analyses. The cardiac tissue is modelled both in a monodomain and a bidomain setting through the rheology, which mimics the response of an orthotropic, hyperelastic, viscous and active material [2, 3], see Figure 1. In the numerical examples, we use virtualized heart geometries generated from cardiac magnetic resonance imaging (cMRI) and echocardiography data and apply physiological boundary conditions. As demonstrative examples, we simulated a left ventricle (LV) and biventricle geometry.

## Cardiac electromechanics

The cardiac tissue is assumed to be a continuum body having five independent sets of field variables

$$\text{State}(\boldsymbol{X},t) := \{\boldsymbol{\varphi}(\boldsymbol{X},t), \Phi_i(\boldsymbol{X},t), \Phi_e(\boldsymbol{X},t); \boldsymbol{\mathcal{I}}_{va}(\boldsymbol{X},t), \boldsymbol{\mathcal{I}}_e(\boldsymbol{X},t)\}\,. \tag{1}$$

The global fields, which are the deformation map $\boldsymbol{\varphi}(\boldsymbol{X},t)$, the intracellular potential $\Phi_i(\boldsymbol{X},t)$ and the extracellular potential $\Phi_e(\boldsymbol{X},t)$, are related to the macroscopic motion and current conduction in the myocardium. Furthermore, the local fields $\boldsymbol{\mathcal{I}}_{va}(\boldsymbol{X},t)$ and $\boldsymbol{\mathcal{I}}_e(\boldsymbol{X},t)$ represent the micro-motion due to the visco-active deformation and the micro-diffusion due to ion concentration differences across the cell membrane, respectively. The electromechanical state is governed by the conservation of linear momentum

$$\boldsymbol{0} = J\ \text{div}\left[J^{-1}\boldsymbol{\tau}\right] + \boldsymbol{b} \tag{2}$$

and conservation of electric charge in the bidomain setting

$$\begin{aligned} \dot{\Phi} &= J\ \text{div}(J^{-1}\boldsymbol{D}_i \cdot \nabla\Phi) + J\text{div}(J^{-1}\boldsymbol{D}_i \cdot \nabla\Phi_e) + F^{\phi}, \\ 0 &= J\ \text{div}(J^{-1}\boldsymbol{D}_i \cdot \nabla\Phi) + J\text{div}(J^{-1}\boldsymbol{D} \cdot \nabla\Phi_e) \end{aligned} \tag{3}$$

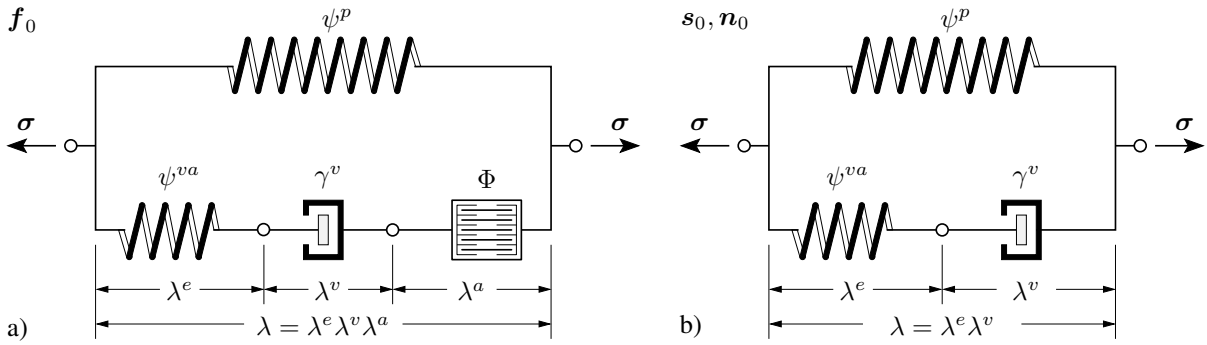


**Figure 1.** Rheology for the electro-visco-elastic response of the myocardium: The upper hyperelastic spring represents the passive response of the myocardium while a) the electro-visco-elastic response is formulated through the elastic spring+dashpot+contractile element in the lower branch for fibre direction $\boldsymbol{f}_0$ and b) the elastic spring+dashpot for the sheet $\boldsymbol{s}_0$ and normal $\boldsymbol{n}_0$ directions.

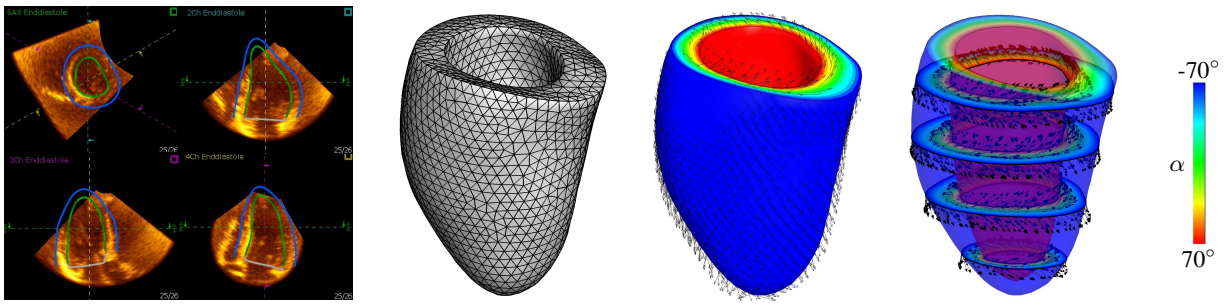


**Figure 2.** From left to right, identification of the endocardial and epicardial surfaces of LV from 4D echo data, discretized LV geometry and two different views of fibre orientation angle $\alpha$.

in a deformable body $\mathcal{B}$ with volume-specific body forces $\boldsymbol{b}$, Jacobian $J$, transmembrane potential $\Phi := \Phi_i - \Phi_e$ and conductivity tensor $\boldsymbol{D} = \boldsymbol{D}_i + \boldsymbol{D}_e$, where $\boldsymbol{D}_i$ and $\boldsymbol{D}_e$ are, respectively, intra and extracellular deformation dependent anisotropic conductivities. The Kirchhoff stress is decomposed into passive and visco-active parts $\boldsymbol{\tau} = \boldsymbol{\tau}^p + \boldsymbol{\tau}^{va}$. The former contribution is described by the orthotropic hyperelastic model [8] while the latter one arises as a result of active (myocardial contraction) and viscous deformation [2]. Moreover, the source term is described by Fitzhugh-Nagumo type excitation equation and has two contributions $F^\phi = F_e^\phi + F_m^\phi$, where the purely electrical part $F_e^\phi$ stands for the ion transmission between the intracellular and extracellular media that is merely triggered by the excitation of nearby cells above a threshold potential value and the mechanical part $F_m^\phi$ is generated upon the stretch of the tissue that induces extra ion transmission through the cell membrane. For a more detailed discussion on theory and implementation, we refer to our previous publications [1–4, 6, 7].

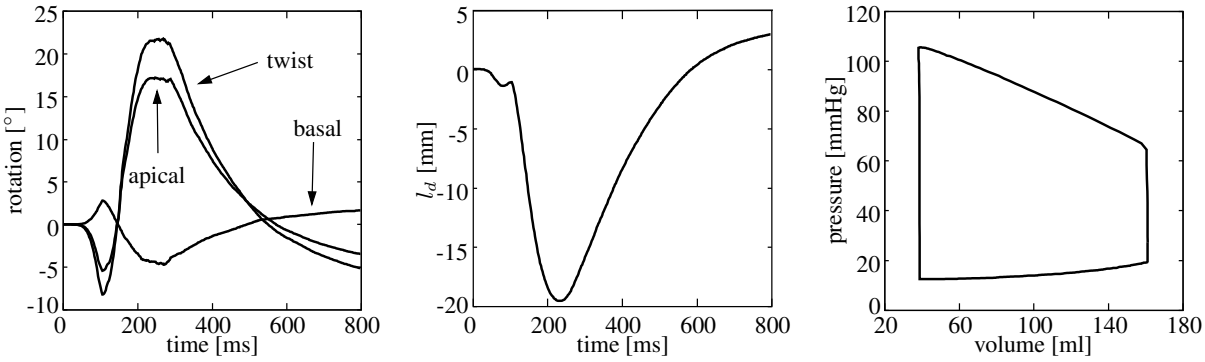


**Figure 3.** From left to right, the rotation of basal and apical regions and twist on the endocardial surface, longitudinal displacement between the peak point of base and apex and pressure-volume relation of LV.

## Numerical examples

This section is devoted to the finite element analysis of virtualized heart models obtained from healthy male humans. In the first example, we utilized a LV geometry that is depicted in Figure 3 with the aim to capture basic characteristics of LV motion during a regular cardiac cycle. In order to initiate depolarization of the LV, a small amount of stimulus is applied to the upper part of the septum corresponding to the atrioventricular node. The constrained state of the ventricles is mimicked by attaching linear springs to the nodes at basal and epicardial surface with $k_x = k_y = k_z = 10^{-4}$ N/mm. In Figure 3 from left to right, we demonstrate the rotation of basal and apical regions and twist on the endocardial surface, longitudinal displacement between the peak point of base and apex and pressure-volume relation of LV. We segmented the endocardial surface into 3 pieces along the longitudinal direction from base to apex, respectively, basal, mittle and apical regions. The basal and apical rotation are calculated by averaging the nodal values over the corresponding region. The graphs reveal that the basal and apical regions rotate in different directions thereby a twist is created, which is essential to pump out the blood in an efficient way. Another important observation is the longitudinal shortening along the long axis that emerges from downward (towards apex) basal motion and upward apical motion. These two results are consistent with physiological motion of LV and in clinical routine [5], rotation and longitudinal shortening are considered as important markers indicating the LV function. It is noteworthy to mention that applied constraints play a crucial role in achieving physiological motion of LV.

In the second example, Figure 4, we simulated a regular heart beat, arrhythmia and termination of arrhythmia by applying an external shock (defibrillation) and recorded corresponding ECG and LV $v-$

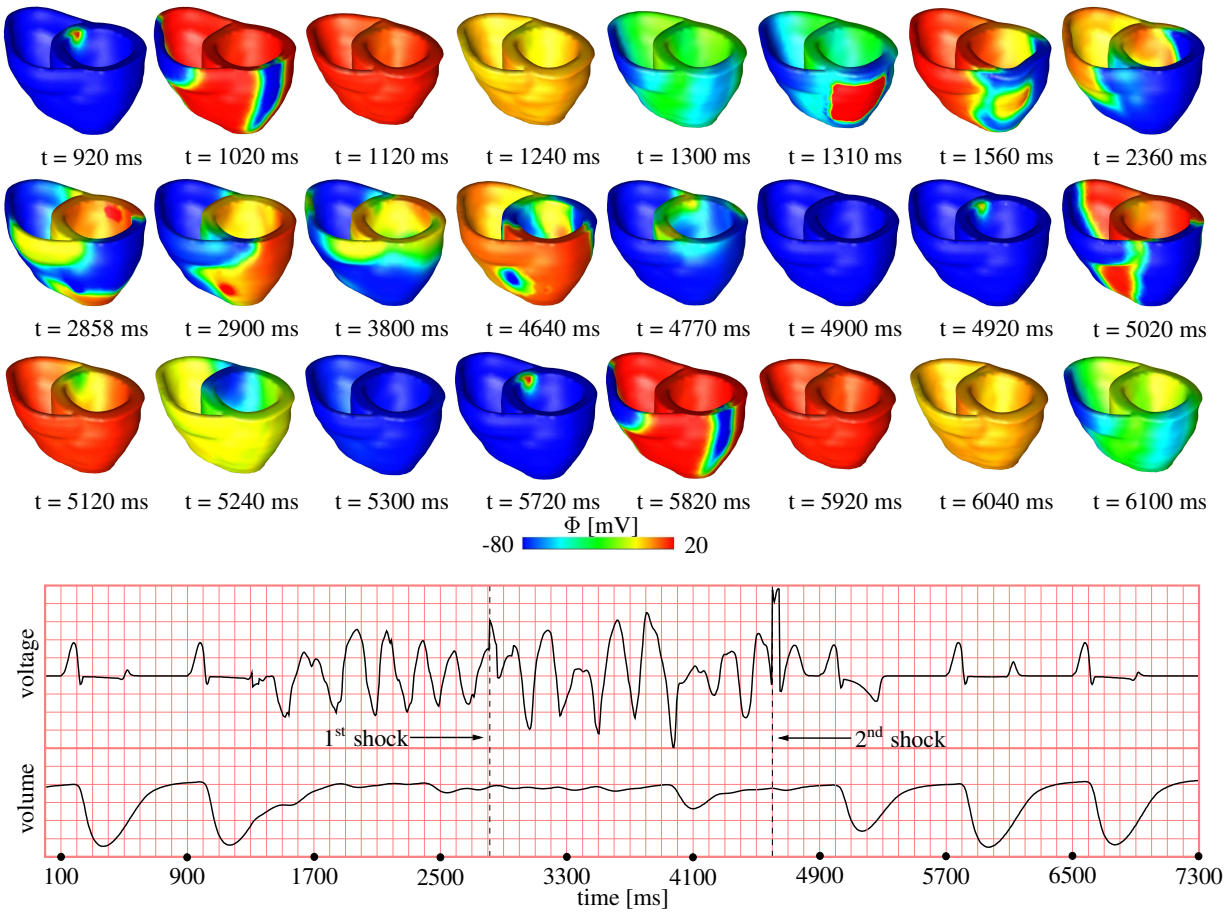


**Figure 4.** Demonstration of regular heart beat, arrhythmia and its termination by an externally applied electrical field. After the first regular beat, the wave propagation is disturbed at time $t = 1310$ ms and eventually turns into a life threatening arrhythmia. In the snapshots, the transmembrane potential distribution is shown and the graph demonstrates ECG, normalized voltage (upper curve), and LV $v - t$ diagram, normalized volume (lower curve), recorded during the simulation.

$t$ curve in a virtualized biventricular heart model. For detailed information on simulation procedure, utilized material parameters, geometry and boundary conditions, we refer to Cansız et al. [3]. Upon the initiation of the arrhythmia, disordered deflections with varying magnitude and formation are observed in ECG. As a result, the myocardial contractility is reduced and the LV output descends to almost zero indicating that the blood cannot be circulated in the body anymore. In order to terminate this life-threatening arrhythmia, we applied an external shock at time $t = 2810$ ms, which was not successful. Thereafter, the second defibrillation attempt at time $t = 4600$ ms could terminate the unsynchronized electrical activity in the ventricles and regular form of ECG and LV $v - t$ is recovered.

## Conclusions

We presented a FE based numerical framework in order to analyse virtualized heart models. The electromechanical state of the cardiac tissue is governed by the conservation of linear momentum and electrical current. On material level, the myocardium is deemed as orthotropic, hyperelastic, viscous and active material. In addition, we generated heart models from cMRI and echocardiography data, which is vital to achieve patient-specific computer simulations. We employed the developed framework in order to imitate the physiological LV motion. The simulation results revealed that setting of boundary conditions is very critical in achieving realistic LV motion and must be further investigated for several virtualized heart models. Moreover, we simulated arrhythmia and its termination (defibrillation) in a virtualized biventricle heart model.

## Acknowledgements

We gratefully acknowledge the financial support of the German Research Foundation (DFG) under grant KA 1163/18.

## References

[1] B. Cansız, H. Dal, and M. Kaliske. Fully coupled cardiac electromechanics with orthotropic viscoelastic effects. *Procedia IUTAM*, 12:124–133, 2015.

[2] B. Cansız, H. Dal, and M. Kaliske. Computational cardiology: A modified hill model to describe the electro-visco-elasticity of the myocardium. *Computer Methods in Applied Mechanics and Engineering*, 315:434–466, 2017.

[3] B. Cansız, H. Dal, and M. Kaliske. Computational cardiology: the bidomain based modified hill model incorporating viscous effects for cardiac defibrillation. *Computational Mechanics*, submitted.

[4] F. B. C. Cansız, H. Dal, and M. Kaliske. An orthotropic viscoelastic material model for passive myocardium: theory and algorithmic treatment. *Computer Methods in Biomechanics and Biomedical Engineering*, 18:1160–1172, 2015.

[5] I. Codreanu, M. D. Robson, S. J. Golding, B. A. Jung, K. Clarke, and C. J. Holloway. Longitudinally and circumferentially directed movements of the left ventricle studied by cardiovascular magnetic resonance phase contrast velocity mapping. *Journal of Cardiovascular Magnetic Resonance*, 12:48, 2010.

[6] H. Dal, S. Göktepe, E. Kuhl, and M. Kaliske. A fully implicit finite element method for bidomain models of cardiac electrophysiology. *Computer Methods in Biomechanics and Biomedical Engineering*, 15:645–656, 2012.

[7] H. Dal, S. Göktepe, E. Kuhl, and M. Kaliske. A fully implicit finite element method for bidomain models of cardiac electromechanics. *Computer Methods in Applied Mechanics and Engineering*, 253:323–336, 2013.

[8] G. A. Holzapfel and R. W. Ogden. Constitutive modelling of passive myocardium: a structurally based framework for material characterization. *Philosophical Transactions of the Royal Society A: Mathematical, Physical and Engineering Sciences*, 367:3445–3475, 2009.